



Experimental Investigation and CFD Modelling of Settling Efficiency in a Cylindrical Tank

G. Isenmann^{1†}, M. Dufresne^{1,2}, J. Vazquez^{1,2}, R. Mosé^{1,2} and C. Fagot³

¹ National School for Water and Environmental Engineering of Strasbourg (ENGEES), Strasbourg, Bas-Rhin, 67000, France

² Mechanics Department, ICube Laboratory, University of Strasbourg, Bas-Rhin, 67000, France

³ ACO, Eure, 27940, France

†Corresponding Author Email: gilles.isenmann@engees.unistra.fr

(Received September 14, 2020; accepted November 4, 2020)

ABSTRACT

Evaluating the performance of a settling tank is an important issue for wastewater system managers. The relevance of a CFD approach for determining the settling efficiency of a tank has already been demonstrated from experimental data obtained from scale models of basins. The CFD modelling strategy is based on the resolution of Navier-Stokes equations to calculate the flow (Eulerian approach), and then on a Newton equation to calculate particle trajectories (Lagrangian approach). In this study, experimental data on settling efficiency are collected in a 1 scale cylindrical settling tank constructed in the laboratory. Eighteen experiments were carried out to collect data (settling efficiency) for a range of flow rates (between 5 and 30 l/s) and three materials representative of the sediments encountered in sewage networks. These data were then compared with the results obtained by CFD modelling to assess the relevance of the numerical approach for a full-scale structure.

Keywords: CFD; Particle tracking; Settling tank; Experimental pilot; Settling efficiency.

1. INTRODUCTION

The decontamination of rainwater flowing over urban surfaces is a new and very important challenge for urban planners. To this end, many depollution devices, essentially based on the principles of settling (sometimes with filtration), have been put on the market by manufacturers: simple settlers, lamellar settlers, hydrodynamic separators, etc. It is essential for planners to evaluate the performance of these systems so that they can choose the system best-adapted to their objectives of decontaminating suspended solids. Several experimental protocols have been devised to this end (see for example the [New Jersey Department of Environmental Protection Laboratory 2013](#); the [Toronto and Region Conservation Authority, 2014](#)). The main difficulty of these protocols is the implementation of scale 1 experiments, which represents a significant cost for large devices.

A promising alternative is the use of CFD modelling. For several years now, much progress has been made in modelling the settling

phenomenon. [Stovin and Saul \(1996, 1998\)](#) showed the potential of the Lagrangian particle tracking approach to assess settling in a basin; in particular, they demonstrated the advantage of a deposition condition based on shear stress. Based on this work, [Dufresne et al. \(2009\)](#) showed that turbulent kinetic energy takes better account of the complexity of the deposition and resuspension phenomenon. [Yan \(2013\)](#) was the first to propose a method to quantify the threshold value of turbulent kinetic energy without relying on experimentation. [Isenmann et al. \(2017\)](#) finally proposed a condition based on turbulent kinetic energy and the approach of [Van Rijn \(1984\)](#), which allows accurately reproducing the deposition of suspended solids for different flow conditions acquired in the laboratory without any calibration. To validate this approach for scale 1, a number of tests with a device whose size is similar to real-life devices are necessary.

This is the subject of this article which proposes, after a description of the experimental set-up and then of the numerical model, a comparison between the experimental and numerical results.

Table 1 Characteristics of the sediments

Sediments	Size (μm)			Density	Settling velocity (m/h)		
	d_{10}	d_{50}	d_{90}		w_{10}	w_{50}	w_{90}
Poraver 100-300	115	215	308	1.24	10.1	18.3	35.9
Poraver 45-125	49	97	130	1.40	3.4	6.4	13.1
Sand 350 Mesh	38	65	85	3.47	5.8	16.6	32.4

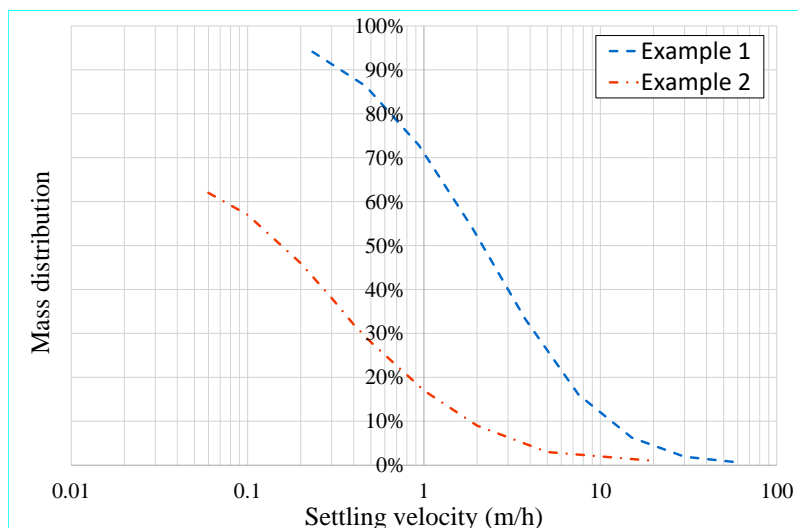


Fig. 1. Examples of settling velocity distributions in rainwater.

2. MATERIALS AND METHODS

2.1 Physical Model

2.1.1. The Sediments

Three materials were used for the experiments: two porous glass beads (Poraver 40-125 and Poraver 100-300) and fine sand (350 Mesh). Their characteristics (size, density, settling velocity) are summarized in Table 1. Densities, particle size distributions and settling velocities were measured with hydrostatic weighting, laser granulometry and acoustic measurements, respectively (see [Isenmann 2016](#) for details).

The sediments used for the tests were selected according to two criteria. On the one hand, they had to be representative of the sediments encountered in stormwater separative systems. On the other hand, they had to be large enough to be easily recoverable downstream of the experimental device. A compromise was found with particles whose settling velocities ranged from 1 to 100 m/h, which roughly corresponds to the coarsest 50% of the sediments (see examples of settling distribution in Fig. 1, which are comparable with those obtained with [Gromaire 2012](#)).

2.1.2. The Experimental Set-Up

The settling tank tested in the laboratory, shown in Fig. 2, is a horizontal cylindrical tank whose size is comparable with real-life settling devices used for stormwater. It has an internal diameter of 2.10 m

and a length of 3.50 m for a volume of 12 m³. The inlet is a circular pipe with a diameter of 0.28 m whose lowest part is located 1.77 m from the bottom of the tank.

The settling tank is first used without any interior baffle and then with a baffle upstream of the outlet pipe. The baffle is located 40 cm upstream of the outlet pipe and starts 1.30 m from the bottom of the tank.

The schematic diagram of the experimental pilot unit is presented in Fig. 3. It is supplied with water by pumping from a 50 m³ storage tank. After pumping, a large part of the flow rate is returned directly to the storage tank and the desired flow rate for the experiment is regulated using a manual control valve. This system ensures the stability of the flow through the settling tank over the duration of the experiment. The flow rate at the inlet of the settling tank is measured by one of the two electromagnetic flowmeters installed upstream of the tank. The first flowmeter (DN65) allows measuring over the flow range 1-25 l/s while the second allows measuring over the flow range 20-60 l/s.

The sediments are prepared in a mixing tank and injected into the inlet pipe of the settling tank. At the outlet, a filtration system recovers the sediments that have not settled into the tank.

The injection device consists of a vertical cylindrical tank in which the mixture of water and sediments is prepared. An agitator is used to

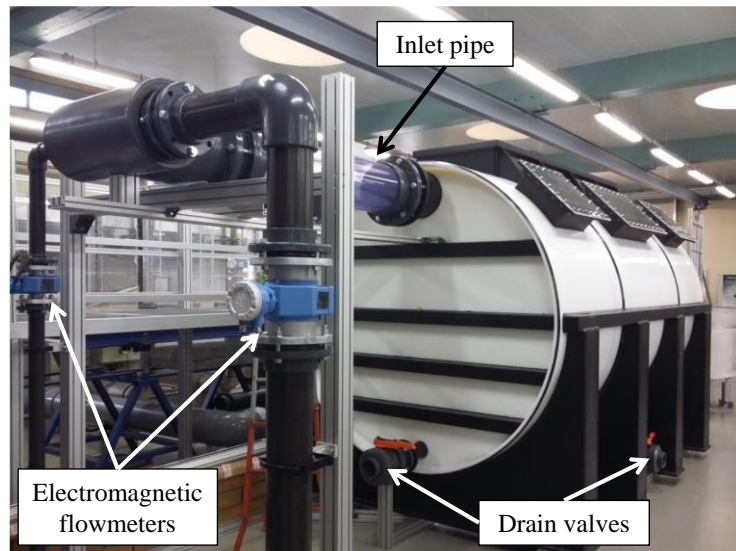


Fig. 2. Experimental settling tank seen from upstream.

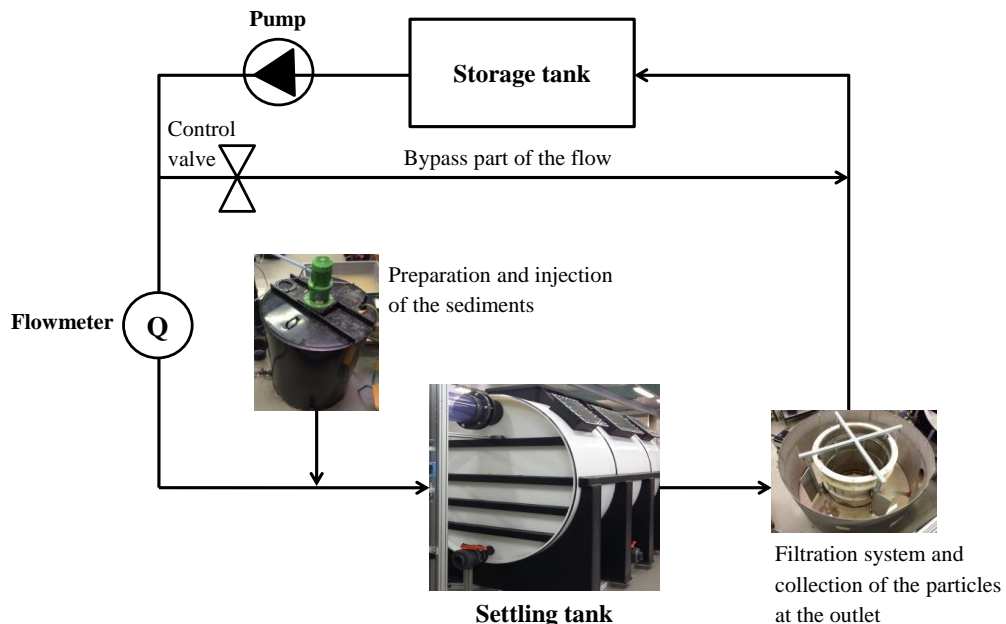


Fig. 3. Schematic diagram of the experimental pilot.

suspend the particles and obtain a homogeneous mixture of a "water+sediment" solution. The order of magnitude of the sediment concentration in the mixing tank is 100 g/l. Injection is then carried out by a peristaltic pump that sends the mixture to a nozzle on the inlet pipe at a constant flow rate. The concentrated mixture is then diluted in the clear water stream feeding the settling tank to reach concentrations of about 300 mg/l (depending on the flow rate of the clear water supply to the settling tank). The consistency of the concentration of particles injected into the settling tank is checked by taking samples downstream of the injection pipe before the start and at the end of injection. The concentration of suspended solids (SS) is measured for each sample. This verifies that the

concentrations at the outlet of the injection device are identical at the beginning and at the end of the experiment. An average difference of 1% and a maximum difference of 4% between the two concentrations is obtained for all the experiments. The homogeneity of the mixture was also checked by comparing the measurements of the SS concentration with the ratio of the mass introduced to the volume of water.

The filtration system installed at the outlet of the settling tank collects the particles that have passed through the settling tank. It is a cylindrical system with a tangential inlet and an outlet at the bottom of the structure in the central part. A 25 μm filter is installed to retain the particles. Rotating brushes are

Table 2 Parameters of the simulations

Hydrodynamic simulation					
Boundary	Inlet	Outlet	Opening on the upper part	Wall and baffle	
Boundary condition	Inlet velocity	Atmospheric pressure	Atmospheric pressure		Standard wall functions
Term	ddtSchemes	grad Schemes	divSchemes: div (rhoPhi,U)	divSchemes: div(rhoPhi,U)	divSchemes: div(phirb,alpha)
Numerical scheme	Euler	Gauss linear	Gauss linear Upwind	Gauss vanLeer	Gauss linear
Particle tracking simulation					
Face	Inlet	Outlet	Opening on the upper part	Wall and baffle	
Boundary condition	Rebound	Escape	Escape	Extended Van Rijn BTKE	
Term	ddtSchemes				
Scheme	Euler				

Table 3 Efficiencies calculated with 1,700,000 and 2,700,000 cells (geometry A and 10 l/s flow rate)

Sediment	Poraver 40 - 125	Poraver 100 - 300	Sand 350 Mesh
1,700,000 cells	72%	84%	86%
2,700,000 cells	69%	83%	85%

used to clean the particles accumulated on the filter during the experiment to prevent the filter from clogging.

2.1.3. Evaluation of Settling Efficiency

For each experiment, the mass of particles injected is obtained from:

- The difference in water level in the mixture tank between the beginning and the end of the experiment (Δh).
- The SS concentration at the outlet of the injection pipe at the beginning (C_1) and at the end of the experiment (C_2). The difference between C_1 and C_2 is on average 1% and a maximum of 4%.

The mass of injected particles M_i is then calculated by the following relationship:

$$M_i = \frac{C_1 + C_2}{2} \cdot \frac{\pi D^2}{4} \cdot \Delta h \quad (1)$$

Where D is the diameter of the mixing tank (1 m).

Two methods were used to determine the settling mass. For some experiments, the quantities of sediments recovered from the bottom of the settling tank are small enough to be put in the oven, dried and weighed. This provides direct knowledge of the mass of material. If the quantity of material is too large to be dried in the oven, the mass of settled sediments is evaluated as follows:

- After the supply to the settling tank has stopped and enough time has elapsed to

remove any suspended particles (about 2 hours), the upper part of the settling tank (clear water) is drained with a pump.

- The sediments are pumped to the mixing tank (previously emptied and rinsed) through an orifice located at the bottom of the settling tank. The settling tank is rinsed with clear water until there are no more particles on the bottom.
- The level of the water in the mixing tank is topped up with clear water if necessary, then measured. This value is noted h_d .
- Agitation is started and a sample is taken to determine the SS concentration of the mixture. It is noted as C_d .

This protocol is justified by the homogeneous nature of the mixture, as mentioned above.

The mass settled on the bottom of the basin during the experiment is then evaluated by the following relationship:

$$M_d = C_d \cdot \frac{\pi D^2}{4} \cdot h_d \quad (2)$$

Finally, the settling efficiency of the tank is calculated by the following relationship:

$$\eta = \frac{M_d}{M_i} \quad (3)$$

The relative error on the settling efficiency is estimated at about 12%.

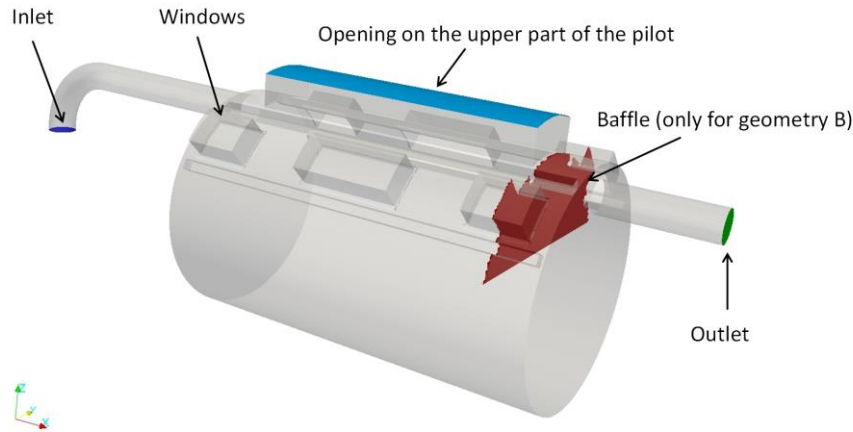


Fig. 4. Geometry of the “empty” tank (geometry A) and with the baffle (geometry B).

2.1.4. Experimental Conditions Studied

Two geometric configurations were studied: the “empty” tank (geometry A) and the tank with a baffle (geometry B). The flow rates studied cover a range between 5 and 30 l/s. Each case tested is represented by the letter corresponding to the geometry and value of the flow rate studied. For example, the experiment for the 10 l/s flow rate on geometry A is noted as A10. For one configuration (A10 and Poraver 40-125), the sensitivity of the results was studied by varying:

- The concentration of the input mixture (noted A10c).
- The duration of the experiment (noted as A10t).

The same experiment was performed again in this configuration to verify the repeatability of the test (noted A10r).

2.2 Numerical Model

2.2.1. Hydrodynamics

The movement of the fluid is described by Navier-Stokes equations (Versteeg and Malalasekera, 2007). For an incompressible fluid, these equations are expressed by a mass conservation equation and a momentum conservation equation. The multiphase water/air nature of the flow is described using the Volume of Fluid method (Hirt and Nichols, 1981), by considering only one fluid whose properties (density and viscosity) vary linearly with the volume fraction α . This parameter is a marker of value 1 in the water phase and 0 in the air phase.

The flows considered in this study are turbulent. The Navier-Stokes equations are averaged with time by applying a Reynolds decomposition for the instantaneous velocity and pressure, and a turbulence model is used to describe the effect of the velocities fluctuating over the mean flow. The $k-\omega$ SST model (Shear Stress Transport) with a standard wall function is chosen. The resolution of

these equations is done using the interFoam solver, available in the library OpenFOAM® (OpenFOAM, 2020). A full description of this solver is provided in Deshpande *et al.* (2012).

2.2.2. Sediment Transport

The movement of a particle in a fluid is described from the Lagrangian viewpoint by resolving the Newton equation (Eq. (4)). Knowing the sum of the forces acting on the particle it is possible to determine the evolution of its position and velocity, or in other terms its trajectory (Maxey and Riley, 1983).

$$m_p \frac{d\mathbf{u}_p}{dt} = \mathbf{F}_D + \mathbf{F}_g + \mathbf{F}_a \quad (4)$$

where m_p = the mass of the particle; \mathbf{u}_p = the velocity of the particle; \mathbf{F}_D = the drag force; \mathbf{F}_g = the apparent weight; and \mathbf{F}_a = the additional forces (pressure gradient, added mass force).

The apparent weight of a particle \mathbf{F}_g corresponds to the force due to the reduced gravity of buoyancy linked to the surrounding fluid. It is expressed by $\mathbf{F}_g = m_p \mathbf{g} (1 - \rho/\rho_p)$ where \mathbf{g} = the gravity acceleration. The additional forces \mathbf{F}_a are not detailed here as they are not considered in what follows due to their negligible impact on the trajectory (Dufresne *et al.* 2009).

Following the use of a RANS model, the turbulent nature of the flow is taken into account by using a random walk model to model the turbulent dispersion of particles. Eddies are created randomly and affect the trajectory of the particles.

The Bed Turbulent Kinetic Energy (BTKE) type condition is used for modelling the behaviour of the particles close to the bottom of the basin (Dufresne *et al.* 2009). The turbulent kinetic energy threshold is calculated as a function of the properties of the particle (diameter and density) as described in Isenmann *et al.* (2017).

The complete description of the particle tracking model is available in Isenmann (2016).

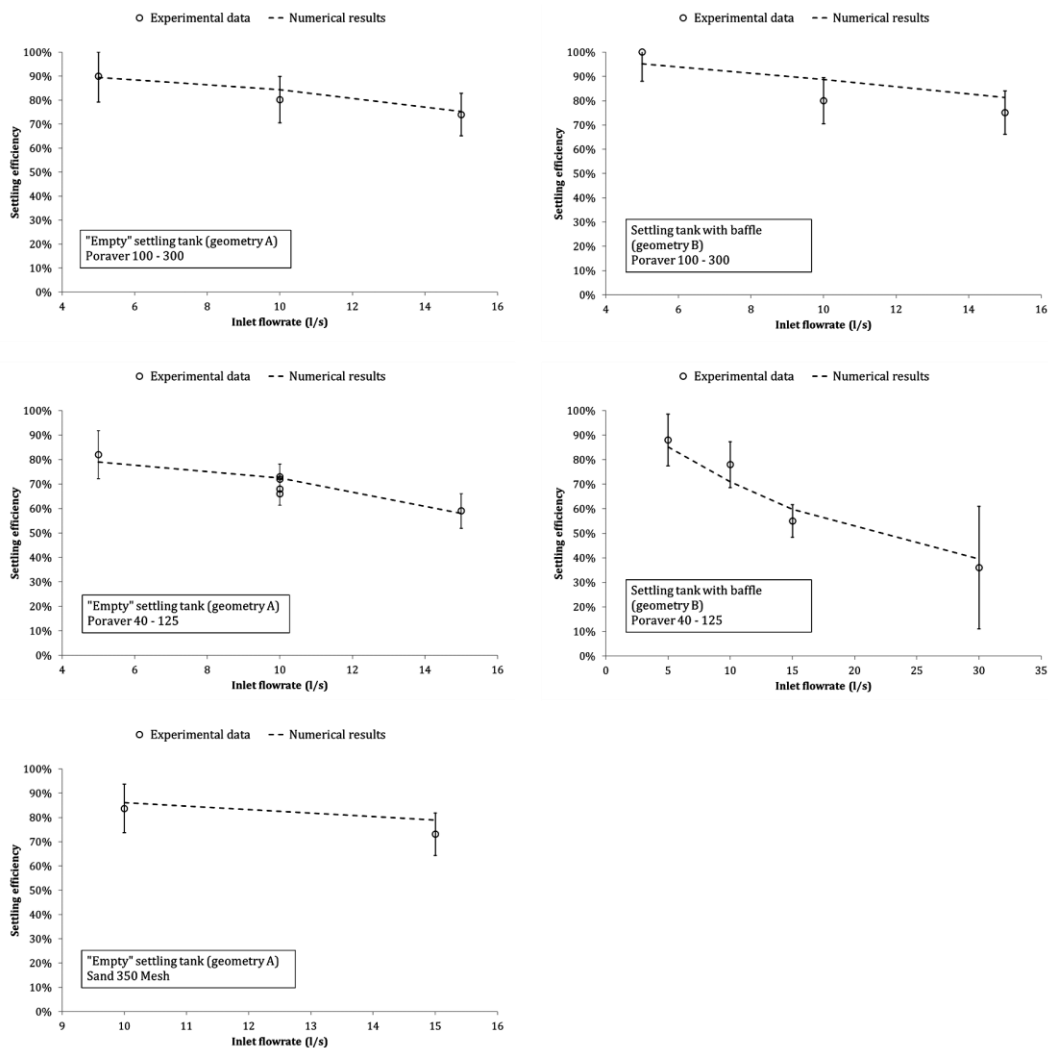


Fig. 5. Comparison of numerical and experimental efficiencies for the three sediments and the two geometries.

2.2.3. Geometry, Meshing and Calculation Parameters

The two geometries studied during the experimental phase are created in 3D. The flow rate is injected over the entire inlet face. The baffle placed during the second phase of the experimental tests is also drawn. The geometry of the “empty” tank (geometry A) and the tank with the baffle (geometry B) are shown in Fig. 4.

The two geometries were meshed using the snappyHexMesh tool (OpenFOAM, 2020). “Cut-cell” type meshes with sides of about 2 cm were chosen (i.e. a y^+ of the order from 50 to 90), leading to a computational domain composed of 1,700,000 cells; this number was chosen after a grid sensitivity analysis. Indeed, a grid size dependence analysis has been performed for geometry A and the 10 l/s flow rate. Simulations have been carried out using 1,700,000 and 2,700,000 cells.

The velocity was imposed on the inlet face of the structure to reproduce the discharges injected

experimentally. The boundary condition at the outlet and on the upper part of the computational domain was an atmospheric pressure. The turbulence model $k-\omega$ SST was used with standard wall functions. The simulated flows are those of the experiments presented above. The convergence of the calculation was checked based on the stability over time of the mass balance at the outlet, and the field of velocities in the different longitudinal and transversal planes.

The particle tracking model presented above was applied to the fifteen geometric and hydraulic combinations. For each sample of particles, a Rosin-Rammler distribution was interpolated to reproduce the experimental grain size distribution. After having verified that this number was sufficient to obtain statistically representative results, ten thousand particles were injected into the hydraulic flow. The densities were fixed at the values measured experimentally: 1400 kg/m^3 for the Poraver 40-125, 1240 kg/m^3 for the Poraver 100-300 and 3470 kg/m^3 for sand (350 Mesh). The forces taken into account to calculate the

trajectories of the particles were drag force and apparent weight. The turbulent nature of the flow was modelled using the stochastic dispersion model. A *rebound* condition was used for the inlet. An *escape* condition (OpenFOAM, 2020) was applied to the outlet and to the atmosphere. The particle/wall interaction “extended Van Rijn BTKE” condition described in Isenmann *et al.* (2017) was used for the walls.

The parameters of the simulations are summarized in Table 2.

When all the particles had been deposited or had left the tank via the outlet, the settling efficiency could be calculated.

3. RESULTS AND DISCUSSION

3.1 Experimental Results

For the “empty” tank and Poraver 100-300 material, the settling efficiency ranged from 90% for the lowest flow rate (5 l/s) to 74% for the 15 l/s flow rate. The efficiencies for this sediment were relatively high, as it had the highest settling velocity.

The settling efficiencies obtained for the Poraver 40-125, still in geometry A, were lower: from 82% (5l/s) to 59% (15 l/s), which is consistent with the material characteristics (the lowest settling velocities studied). The experiment with the intermediate flow rate (10 l/s) was carried out twice with the same parameters (repeatability). Considering the uncertainty, the efficiency values were similar: 72% (A10) and 66% (A10r). This configuration was also used to study the dependence on the duration of the experiment and the input concentration. Efficiencies were found at 73% (A10c) and 68% (A10t), close to the efficiency measured for the A10 configuration (72%), and show the independence of the results with respect to duration and input concentration.

Two flow rates were studied for the 350 Mesh sand in the “empty” settling tank: 10 l/s and 15 l/s. The efficiency values were 84% and 73%. These are of the same order of magnitude as the results obtained for the Poraver 100-300 for identical flow rates, which is consistent since these two materials have relatively similar settling velocities (see Table 1)

The efficiencies obtained with the baffle (geometry B) were of the same order of magnitude as for the “empty” tank. For the Poraver 100-300, the efficiencies ranged from 100% (5 l/s) to 75% (15 l/s). A wider range was studied for the Poraver 40-125: an experiment was carried out for a flow rate of 30 l/s. For this material, the abatement rates ranged from 88% to 36% (30 l/s).

All the experimental results are summarized in Fig. 5.

3.2 Comparison of Numerical and Experimental Results

Figure 5 shows the comparison of numerical and

experimental efficiencies on geometry A (“empty” tank) and geometry B (with baffle) for different flow rates. Each graph corresponds to a material and a geometry.

For the Poraver 40-125, a flow rate of 10 l/s and geometry A, four numerical efficiency values are shown. These values were obtained from the tests performed to study the reproducibility of the experiment, the sensitivity of the results to the duration of the experiment and the concentration at the inlet of the settling tank.

A grid size dependence analysis has been performed for geometry A and the 10 l/s flow rate. In terms of settling efficiencies, the comparison is given in Table 3. For each type of sediment, the maximum deviation is 3%, which is not significant. This study shows that 1,700,000 cells are sufficient for geometry A. We assume that the same type of mesh can be used to obtain accurate results for geometry B and other flow rates.

Regarding all 18 experiments, the absolute difference between the numerical and experimental efficiencies was on average 4% and always within the experimental uncertainty bars. The maximum deviation was 9%. This corresponds to the B10 configuration for the Poraver 100-300.

4. CONCLUSION

After experiments already performed at small scale, the present study focused on carrying out settling tests in a system comparable in size to the devices used for the decontamination of stormwater. The comparison with the results of the CFD model showed very good agreement. These results make it possible to consider using the CFD model to evaluate the settling performance of stormwater decontamination systems based on the settling principle.

ACKNOWLEDGEMENTS

The authors would like to thank Maxime Trautmann and Martin Fischer for their contribution during the experimental phase.

REFERENCES

- Deshpande, S. S., L. Anumolu and M. F. Trujillo (2012). Evaluating the performance of the two-phase flow solver interFoam, *Computational Science and Discovery* 5, 014016.
- Dufresne, M., J. Vazquez, A. Terfous, A. Ghenaïm and J. B. Poulet (2009). Experimental investigation and CFD modelling of flow, sedimentation, and solids separation in a combined sewer detention tank, *Computer and Fluids* 38(5), 1042-1049.
- Gromaire, M. C. (2012). *Contribution à l'étude des sources et flux de contaminants dans les eaux pluviales urbaines* [in french]. PhD Thesis, University Paris Est, Paris, France.

- Hirt, C. W. and B. D. Nichols (1981). Volume of fluid (VOF) method for the dynamics of free boundaries. *Journal of Computational Physics* 39, 201–225.
- Isenmann, G. (2016). *Approche Euler-Lagrange pour la modélisation du transport solide dans les ouvrages de décantation* [in french]. PhD Thesis, University of Strasbourg, Strasbourg, France.
- Isenmann, G., M. Dufresne, J. Vazquez and R. Mosé (2017). Bed turbulent kinetic energy boundary conditions for trapping efficiency and spatial distribution of sediments in basins. *Water Science and Technology* 76(8), 2032-2043.
- New Jersey Department of Environmental Protection Laboratory (2013). New Jersey Department of Environmental Protection Laboratory Protocol to Assess Total Suspended Solids Removal by a Hydrodynamic Sedimentation Manufactured Treatment Device. <http://www.nj.gov/dep/stormwater/pdf/hds-protocol-1-25-13.pdf> (accessed 01 September 2020).
- OpenFOAM. (2000). Official OpenFOAM Repository–GitHub. <https://github.com/OpenFOAM> (accessed 01 September 2020).
- Stovin, V. R. and A. J. Saul (1996). Efficiency prediction for storage chambers using computational fluid dynamics. *Water Science and Technology* 33(9), 163-170.
- Stovin, V. R. and A. J. Saul (1998). A computational fluid dynamics (CFD) particle tracking approach to efficiency prediction. *Water Science and Technology* 37(1), 285-293.
- Toronto and Region Conservation Authority. (2014). Procedure for Laboratory Testing of Oil-Grit Separators.
- Van Rijn, L. (1984). Sediment transport, part I: bed load transport. *Journal of Hydraulic Engineering* 110(10):1431-1455.
- Versteeg, H. K. and W. Malalasekera (2007). *An Introduction to Computational Fluid Dynamics*. Prentice Hall, Harlow, England.
- Yan, H. (2013). *Experiments and 3D modelling of hydrodynamics, sediment transport, settling and resuspension under unsteady conditions in an urban stormwater detention basin*. PhD thesis, Institut National des Sciences Appliquées, Lyon, France.